

## Application of cherry laurel seeds activated carbon as a new adsorbent for Cr(VI) removal

Nurcan Öztürk<sup>\*1</sup>, Murat Yazar<sup>2a</sup>, Ali Gündoğdu<sup>2b</sup>, Celal Duran<sup>3b</sup>, Hasan Basri Şentürk<sup>3b</sup> and Mustafa Soylak<sup>4b</sup>

<sup>1</sup>Department of Civil Engineering, Faculty of Technology, Karadeniz Technical University, 61830 Trabzon, Turkey

<sup>2</sup>Department of Pharmacy Services, Maçka Vocational School, Karadeniz Technical University, 61750 Trabzon, Turkey

<sup>3</sup>Department of Chemistry, Faculty of Science, Karadeniz Technical University, 61080 Trabzon, Turkey

<sup>4</sup>Department of Chemistry, Faculty of Science, Erciyes University, 38039 Kayseri, Turkey

(Received September 4, 2019, Revised January 6, 2021, Accepted January 14, 2021)

**Abstract.** A novel activated carbon produced from cherry laurel (*Laurocerasus officinalis* Roem.) seeds (CLSAC) by chemical activation with  $ZnCl_2$  was used as an adsorbent to remove Cr(VI) ions from aqueous solutions. CLSAC was characterized by several techniques and the adsorption experiments were performed in a batch model adsorption technique. The effects of various experimental parameters were investigated as a function of solution pH, contact time, initial Cr(VI) concentration, CLSAC concentration, and temperature. The monolayer adsorption capacity of CLSAC was found to be  $41.67 \text{ mg g}^{-1}$  for  $5.0 \text{ g L}^{-1}$  of CLSAC concentration and, it was concluded that CLSAC can be used as an effective adsorbent for removal of Cr(VI) from waters and wastewaters.

**Keywords:** chromium(VI); adsorption; isotherms; kinetics; thermodynamics

### 1. Introduction

Rapidly increasing industrialization has produced large volumes of extremely contaminated wastewaters. Industrial effluents containing various heavy metals like chromium, quite toxic for animals and human beings, negatively affect our ecosystem (Hajeeth *et al.* 2014, Al-Othman *et al.* 2012). Numerous industrial processes such as aircraft, steel manufacturing, electroplating, leather tanning, wood preserving, metal finishing, textile, dye, paint and paper manufacturing, cement, textile and photography are main sources of chromium waste released to the environment (Hajeeth *et al.* 2014, Burks *et al.* 2014, Avila *et al.* 2014, Olad *et al.* 2014).

The most common forms of chromium in aqueous phase are trivalent, Cr(III), and hexavalent, Cr(VI), species (Karthik and Meenakshi 2014). The hexavalent chromium, a commonly used heavy metal, is considered as 500 times more toxic, carcinogenic and mutagenic than trivalent chromium (Olad and Farshi Azhar 2014, Kumar *et al.* 2014, Wang *et al.* 2013). The hexavalent chromium generally present in the form of anions, chromate ( $CrO_4^{2-}$ ) and dichromate ( $Cr_2O_7^{2-}$ ), has high oxidation potential, ability to diffuse through cell membranes and modifies DNA transcription process (Yao *et al.* 2014, Rao *et al.* 2014,

DHSS, 1991). Besides, it is reported that short or long term exposure to Cr(VI) causes cancer in the digestive tract and lungs, asthma, epigastric pain, dermatitis, kidney and liver failure, nausea, vomiting and weakened immune system (DHSS, 1991, Mohanty *et al.* 2005, Axtell *et al.* 2003).

The World Health Organization (WHO) restricts the maximum concentration limit for Cr(VI) in potable water as  $0.05 \text{ mg L}^{-1}$  (Vasudevan *et al.* 2010). So, it is essential to control and treat before Cr(VI) discharge into the water bodies.

For removal of Cr(VI) from waters, a variety of conventional methods have been employed including reverse osmosis, chemical reduction, electrochemical reduction, ion exchange, membrane separation, evaporation, adsorption, Donnan dialysis and so forth (Das *et al.* 2006, Alidokht *et al.* 2011, Lakshminathiraj *et al.* 2008, Gode and Pehlivan 2005, Fraser *et al.* 1994, Morisset *et al.* 1955, Sardohan *et al.* 2010). When compared to adsorption, these processes have serious drawbacks like generation of toxic byproducts, high capital, maintenance and operational cost and incomplete removal (Al-Othman *et al.* 2012, Rao *et al.* 2014).

As one of the most effective methods, adsorption technology is usually applied to remove Cr(VI) from wastewater because of its ease of operation, high efficiency, simplicity of design, regeneration ability, fast separation, negligible investment and safety (Karthik and Meenakshi 2014, Yao *et al.* 2014, Park and Jang 2012, Fierro *et al.* 2008).

Recently, researchers have investigated the usage of low-cost and naturally occurring materials as adsorbent to

\*Corresponding author, Ph.D., Assistant Professor  
E-mail: nurcan@ktu.edu.tr

<sup>a</sup> Ph.D. Student

<sup>b</sup> Ph.D., Professor

remove heavy metals (Zhang *et al.* 2018). For this purpose, various agricultural wastes or byproducts had been directly used or converted into activated carbon (AC). AC is the most promising adsorbents because of its unique characteristics (high stability, surface area and adsorption capacity) (Ampiauw *et al.* 2019, Ahmed *et al.* 2020). Commercial AC is relatively expensive materials, but it has high adsorption capacity, hence must be generated from cheaper raw materials. In literature, there are many different type of AC prepared from a variety of materials like waste polyester textiles (Yuan *et al.* 2018), date press cake (Norouzi *et al.* 2018), stems of *Leucas Aspera* (Shanmugalingam and Murugesan 2018), corncob (Li *et al.* 2018), bamboo (Xu *et al.* 2018), coffee waste (Suganya and Senthil Kumar 2018), apple peels (Enniya *et al.* 2018), Brewers' spent grain (Vanderheyden *et al.* 2018), sewage sludge (Aliakbari *et al.* 2017), polyacrylonitrile, Fox nutshell (Kumar and Jena 2017), glycerol (Cui and Atkinson 2017), luffa sponge (Wang *et al.* 2016) and crofton weed (Wang *et al.* 2013).

In production of AC, carbonization in an inert atmosphere and activation processes, physical and chemical, have been applied. The raw material is pyrolyzed and activated at certain temperatures to increase adsorption capacity at the carbonization stage. Physical activation includes carbonization of raw material and then activation in CO<sub>2</sub> or steam atmosphere. In the chemical activation, thermal decomposition of carbonaceous material can be conducted with acidic (ZnCl<sub>2</sub>, H<sub>3</sub>PO<sub>4</sub>, HCl and H<sub>2</sub>SO<sub>4</sub>) or basic (K<sub>2</sub>CO<sub>3</sub>, KOH and Na<sub>2</sub>CO<sub>3</sub>) activating agents. In a previous study, ACs of cherry laurel stone with KOH activation were produced and applied for CH<sub>4</sub> and H<sub>2</sub> adsorption with high microporous structure and high surface area (Toprak 2020).

In the present work, ZnCl<sub>2</sub> is used as an activating agent for chemical activation of cherry laurel (*Laurocerasus officinalis* Roem.) seeds (CLS) and produced AC named CLSAC. Usage of ZnCl<sub>2</sub>, a well-known dehydrating reagent, provides extended surface area and more porous structure, thus increases adsorption efficiency of the materials (Khalilia *et al.* 2000). *L. officinalis* grows southwestern Asia and southeastern Europe. In Turkey's certain cities like Trabzon, Giresun, Ordu, Rize and Artvin, it is naturally found. *L. officinalis*, locally named "karayemiş" and also called "Taflan" or "wild cherry" in these regions, has diuretic and antidiabetic properties. Production of *L. officinalis* obtained from one decares garden is about 3 tons. Its seeds are not used in any industrial or other fields in Turkey. So, AC production from seeds of the abundant fruits, and investigation of adsorption capacities of them to remove Cr(VI) and also other organic and inorganic pollutants from aqueous solutions are an essential application in terms of economic and environmental issues.

After CLSAC was produced by ZnCl<sub>2</sub> activation, it was characterized by various techniques such as FT-IR, SEM, iodine and methylene blue numbers, pore texture, pH of point zero charge (pH<sub>PZC</sub>) and elemental analysis. Then, a batch adsorption system was conducted for the removal of Cr(VI) by the CLSAC. The influences of various operating parameters like pH, amount of CLSAC, contact time, initial

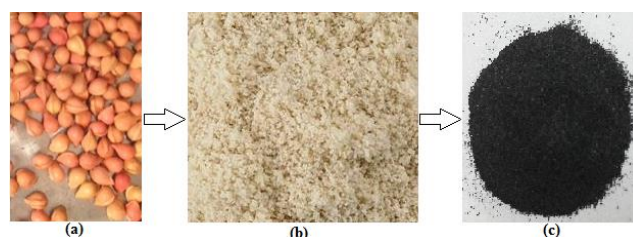


Fig. 1 Picture of (a) CLS, (b) ground CLS, (c) CLSAC activated by ZnCl<sub>2</sub> (final AC)

Cr(VI) concentration, temperature, etc., were studied in this paper. The adsorption mechanisms of Cr(VI) onto CLSAC were evaluated thermodynamically and by different kinetic models. The adsorption isotherm models, Langmuir and Freundlich, were also used to explain equilibrium data.

## 2. Materials and methods

### 2.1 Equipments

Autosorb-1-C/MS (Quantachrome Corporation) model specific surface area analyzer was used to determine CLSAC's specific surface area. The FT-IR spectrum of the CLSAC was recorded between 450 and 4000 cm<sup>-1</sup> in a Perkin Elmer Frontier ATR-FTIR spectrometer. SEM analyses were applied using Zeiss Evo LS-10 apparatus. Elemental analysis of CLSAC was performed on a LECO, CHNS-932 apparatus. A Perkin Elmer model AAnalyst-400 Flame Atomic Absorption Spectrometer (FAAS) with deuterium background corrector was used for the chromium determination in solutions. Edmund Bühler GmbH model mechanical shaker was used for batch adsorption experiments. The pH measurements were made on Hanna pH-211 (HANNA instruments/Romania) digital desktop pH meter. Thermodynamic studies were performed on a Nüve BD-402 model water bath providing temperature control of solutions for uniform and stable temperature. Distilled/deionized water was obtained from Sartorius Milli-Q system (arium® 611UV).

### 2.2 Chemicals

All chemicals used were analytical grade (>95% pure) of Merck (Darmstadt, Germany) and Fluka (Buchs, Switzerland). The working solutions of Cr(VI) for batch adsorption were prepared by diluting from 1000 mg L<sup>-1</sup> Cr(VI) solution with Milli Q water. Distilled/deionized water was used for all experiments.

### 2.3 Preparation of CLSAC

In present study, Cherry laurel seeds (CLS) was used to produce AC, and it was provided from Black Sea Region of Turkey (Trabzon) (Fig. 1 (a)). Before production AC, CLS were first cut in to small pieces and then dried in an oven at 105 °C for 20 h (Fig. 1 (b)) The dried CLS was used for AC preparation by chemical activation with ZnCl<sub>2</sub> depending on activating agent: CLS ratio selected as 1:1 w/v and

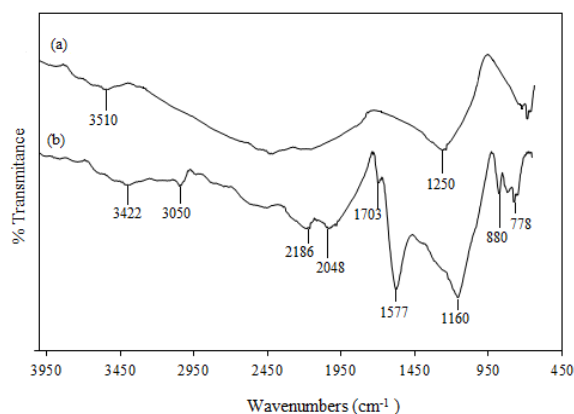


Fig. 2 FT-IR spectra of (a) CLSC obtained only by carbonization and (b) CLSAC activated by  $ZnCl_2$

keeping it at 500 °C under  $N_2$  atmosphere for 4 h. This carbonized material was boiled within 2 M HCl to remove any impurities, filtrated through vacuum filtration setup, and washed thoroughly with distilled water for several times to remove the free acid. Then the AC obtained was dried at 105 °C in a hot air oven for 4 h and then ground and sieved to the particle size of 150  $\mu m$  (Fig. 1 (c)).

#### 2.4 Batch adsorption procedure

Batch adsorption experiments were carried out by optimizing the operation conditions for Cr(VI) adsorption onto CLSAC. In a typical experiment, 10 mL of Cr(VI) solution in the concentration range of 100–1000  $mg L^{-1}$  was transferred into a 15 mL polyethylene centrifuge tube. Then, 50 mg of CLSAC (5  $g L^{-1}$ ) was added to the solution and content was agitated on a mechanical shaker at 400 rpm for 4.0 h. The experiments were repeated at 5, 15, 25, 40 °C. After equilibrium, the phases were separated by filtration and the Cr(VI) concentration in the filtrate was determined by FAAS. Adsorption parameters such as initial pH of Cr(VI) solution, initial concentration of Cr(VI), contact time, adsorbent dosage and temperature were optimized by continuous variation method. For pH optimization, the initial pH of each Cr(VI) solution was adjusted to the required pH by addition of 0.1 M HCl or NaOH solutions. Throughout the study, the pH was varied from 1 to 10, the initial Cr(VI) concentration from 100 to 1000  $mg L^{-1}$ , the contact time from 1 to 720 min, and the adsorbent dosage from 1 to 20  $g L^{-1}$ .

The percent adsorption metal ion was calculated as follows:

$$Adsorption(\%) = \frac{(C_o - C_e)}{C_o} \times 100 \quad (1)$$

where  $C_o$  and  $C_e$  are the initial and the equilibrium Cr(VI) concentrations ( $mg L^{-1}$ ), respectively.

The adsorption capacity was calculated using the following formula:

$$Q_e = \frac{(C_o - C_e)V}{W} \quad (2)$$

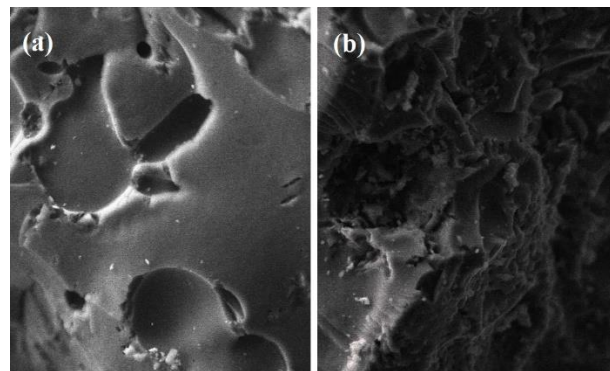


Fig. 3 SEM micrographs of (a) CLSC and (b) CLSAC (magnification: 2000 folds)

where  $Q_e$  is the amount of metal ion adsorbed on the adsorbent ( $mg g^{-1}$ ),  $V$  is the volume of metal ion solution used (L), and  $W$  is the mass of dry adsorbent used (g).

#### 2.5. Desorption procedure

For desorption studies, Cr(VI) was initially adsorbed on the CLSAC at pH 2.5 and the equilibrium concentration of Cr(VI) in the solution was measured, then the system was filtered. After 10 mL NaOH solutions (concentration of them varied from 0.1 to 5.0 M) were added separately to the filters in the centrifuge tubes, contents in the tubes were agitated again at 400 rpm for 4.0 h to desorb the adsorbed Cr(VI) onto CLSAC. The equilibrium concentration after desorption was determined by FAAS.

### 3. Results and discussion

#### 3.1 Characterization of CLSAC

The chemical structure and functional groups of AC can define its adsorption capacity. For this purpose, the infrared spectrums (450–4000  $cm^{-1}$ ) of CLSC (only carbonized material) (a) and CLSAC (activated by  $ZnCl_2$ ) (b) were depicted in Fig. 2. A previous characterization study revealed that fatty acids such as oleic, linoleic and palmitic acid were found to be major volatile compounds in CLS (Elmastas *et al.* 2013). During carbonization, non-carbon elements were removed from CLS, the carbon content of high volatility CLS was increased, its volatility was reduced, and a more regular carbon skeleton was formed. Hence, IR spectrum of CLSC obtained by carbonization at high temperatures is very much simpler. The most significant peaks for CLSC are at 3510 and 1250  $cm^{-1}$  indicating the presence of –OH and C–O group, respectively (Fig. 2 (a)). In the Fig. 2 (b), the broad peak observed at 3422  $cm^{-1}$  is due to stretching vibrations of the bonded hydroxyl (–OH) groups present in the sample. Three peaks at 3050  $cm^{-1}$ , 2186  $cm^{-1}$  and 2048  $cm^{-1}$  arise from the aromatic =C–H groups existing in the structure. The peak appearing at 1703  $cm^{-1}$  is C=O group due to carboxyl group. The long peaks at 1577 and 1160  $cm^{-1}$  point to existence of carboxylic acid and/or lactone group and C–O group, respectively. The peaks at 880 and 778  $cm^{-1}$  also indicate aromatic structure.

The Scanning electron microscopy (SEM) analyses were conducted on CLSC and ZnCl<sub>2</sub> activated CLSAC to visualize the surface structure and morphology of the adsorbents. In the carbonized product (CLSC), it can be seen no porous structures (Fig. 3 (a)). As shown in Fig. 3 (b), the shape of CLSAC seems to be formed by rough scaly sheets and it has indents and protrusions.

The results of the BET (Brunauer-Emmett-Teller) surface area ( $S_{BET}$ ),  $t$ -plot micropore area ( $S_{micro}$ ), mesopore area ( $S_{meso}$ ), total pore volume ( $V_t$ ), micropore volume ( $V_{micro}$ ) and average pore diameter ( $D_p$ ) calculated from  $4V_t/S_{BET}$  formula for CLSAC were listed in Table 1. Percentage amount of moisture, volatile matter, fixed carbon, ash and C, H, N, S and O contents obtained from the elemental analysis of CLSAC was given in Table 1. The quantity of acidic functional groups affecting adsorption capacity on CLSAC surface were determined and listed in Table 1. Methylene blue and iodine numbers can give an idea about the mesopore and micropore (pore diameter lower than 1nm) structures respectively, were defined (ASTM D4607-94(1999) 2006). CLSAC's pH value and value of  $pH_{PZC}$  were determined. The  $pH_{PZC}$  is the pH value at which net surface charge of the adsorbent is neutral (Mestre *et al.* 2007). The surface charge of CLSAC was negative at  $pH > pH_{PZC}$ , while it was positive at  $pH < pH_{PZC}$ .

### 3.2 Effect of solution pH

The pH of the solution is an important parameter affecting the activity of the functional groups on the adsorbent surface and the competition of metal ions to get adsorbed to the active sites. The effect of pH on the adsorption of Cr(VI) onto CLSAC was investigated in the pH range of 1–10 using 10 mL of model solutions containing 5.0 g L<sup>-1</sup> of CLSAC suspension for 4.0 h as shown in Fig. 4. The experimental results revealed that the adsorption efficiency was higher at low pH range (2.0–4.0) and the maximum adsorption of Cr(VI) took place at pH 2.5. Because hexavalent chromium presents different ionic forms at different pH conditions, the existence and stability of it depends on the pH of the solution medium. The different Cr(VI) species such as H<sub>2</sub>CrO<sub>4</sub>, HCrO<sub>4</sub><sup>-</sup>, CrO<sub>4</sub><sup>2-</sup>, and Cr<sub>2</sub>O<sub>7</sub><sup>2-</sup> exist at acidic pH values and the hydrochromate anion (HCrO<sub>4</sub><sup>-</sup>) converted to CrO<sub>4</sub><sup>2-</sup> species as the solution pH increases predominates in the pH range (higher adsorption efficiency range in Fig. 4) 2.0–4.0. The concentration of HCrO<sub>4</sub><sup>-</sup> and the adsorption of Cr(VI) onto CLSAC decreased with the increase in solution pH (Fig. 4). The variation in adsorption of Cr(VI) at different pH values may be attributed to the affinities of CLSAC for the different Cr(VI) species (Burks *et al.* 2014, Benefield *et al.* 1982, Karthikeyan *et al.* 2005). The influence of pH for the adsorption of Cr(VI) onto CLSAC could also be explained based on the development of surface charge of CLSAC in acidic/alkaline pH. At lower pH, the adsorbent surface is charged positively and the oxyanions of Cr(VI) interact electrostatically with positively charged adsorbent active sites. However, the negative charged surface occurs at higher pH and leads to electrostatic repulsion between the species of Cr(VI) and the surface. As a result, the amount of Cr(VI) adsorption decreases with the increase in solution

Table 1 Characteristics of CLSAC

Pore structure of CLSAC	
$S_{BET}$ (m <sup>2</sup> g <sup>-1</sup> )	1051.4
$S_{micro}$ (m <sup>2</sup> g <sup>-1</sup> )	167.5
$S_{meso}$ (m <sup>2</sup> g <sup>-1</sup> )	883.9
$V_t$ (cm <sup>3</sup> g <sup>-1</sup> )	1.61
$V_{micro}$ (cm <sup>3</sup> g <sup>-1</sup> )	0.096
$D_p$ (nm)	6.13
Elemental analysis (wt%)	
C	80.92
H	3.091
N	2.583
S	0.079
O <sup>a</sup>	13.33
Surface functional groups (mmol g <sup>-1</sup> )	
Carboxylic	1.64
Phenolic	0.60
Lactonic	0.22
Total acidic value	2.46
Proximate analyses (wt%)	
Moisture	3.35
Volatile matter	19.18
Fixed carbon	79.4
Ash	1.41
Iodine number (mg g <sup>-1</sup> )	520.38
Methylene Blue number (mg g <sup>-1</sup> )	501.33
pH	5.69
$pH_{PZC}$	5.01

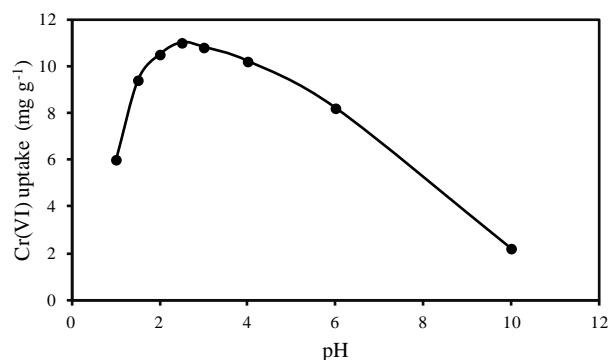


Fig. 4 Effect of pH on the adsorption of Cr(VI) by CLSAC (Initial Cr(VI) conc.: 100 mg L<sup>-1</sup>, CLSAC conc.: 5.0 g L<sup>-1</sup>, contact time: 4.0 h; agitation speed: 400 rpm, N=3, RSD=<5%)

pH (Kumar *et al.* 2014, Levankumar *et al.* 2009, Cui *et al.* 2013). In addition, the point of zero charge ( $pH_{PZC}$ ) of CLSAC helps deciding the pH of the solution during adsorption studies. While adsorption of cation is favored at  $pH > pH_{PZC}$ , the adsorption of anions is favored at  $pH < pH_{PZC}$

(Srivastava *et al.* 2008, Hizal and Apak 2006). This is evidence why there is a significant increase in adsorption by CLSAC in the pH range 2.0–4.0 so all subsequent experiments were performed at pH 2.5.

### 3.3 Effect of contact time and kinetics of Cr(VI) adsorption

The effect of contact time on the adsorption Cr(VI) ions onto CLSAC was investigated in the time ranges of 1–720 min by contacting 100 mg L<sup>-1</sup> of Cr(VI) solutions at initial pH 2.5 with 5.0 g L<sup>-1</sup> of CLSAC suspensions to decide whether the equilibrium was reached. It was observed that Cr(VI) adsorption rate is high at the beginning of the adsorption because of more available adsorption sites easily adsorbing Cr(VI) ions and then Cr(VI)–CLSAC interactions reached equilibrium at 4.0 h (Fig. 5). A larger amount of Cr(VI) was adsorbed (17.5 mg g<sup>-1</sup>) in the first 30 min of contact time and Cr(VI) adsorption become constant after 4.0 h. Thus, the contact time of 4.0 h was used in the following adsorption experiments.

Various kinetic models, pseudo-first-order, pseudo-second-order and intraparticle diffusion model were applied for the experimental data to evaluate the adsorption kinetics of Cr(VI) onto CLSAC.

The pseudo-first-order kinetic model, the most popular model, is described in Eq. (3):

$$\ln(q_e - q_t) = \ln q_e - k_1 t \quad (3)$$

where  $q_e$  (mg g<sup>-1</sup>) is the amount of adsorption equilibrium;  $q_t$  (mg g<sup>-1</sup>) is the amount of adsorption time  $t$  (min);  $k_1$  (min<sup>-1</sup>) is the rate constant of the first order model. The value of  $q_e$  and  $k_1$  can be determined experimentally from the intercept and slope of the  $\ln(q_e - q_t)$  versus  $t$  plot, respectively. The determined  $q_e$ ,  $k_1$  and correlation coefficient ( $r^2$ ) values were shown in Table 2. Since the value of  $r^2$  was low and  $q_e$  (exp) determined from experimental values and  $q_e$  (cal) determined from the model were not in a good agreement, pseudo-first-order kinetic model was not suitable for modeling the adsorption of Cr(VI) onto CLSAC.

The pseudo-second-order kinetic model is presented in Eq. (4):

$$\frac{t}{q_t} = \frac{1}{k_2 q_e^2} + \frac{t}{q_e} \quad (4)$$

where  $q_t$  (mg g<sup>-1</sup>) is the amount of adsorption time  $t$  (min);  $q_e$  (mg g<sup>-1</sup>) is the maximum adsorption capacity;  $k_2$  (g mg<sup>-1</sup>min<sup>-1</sup>) is the rate constant of the second order equation. As seen in Fig.4(b), the linear plot of  $t/q_t$  versus  $t$  for pseudo second order model in Eq. (4) was obtained and the plot giving a straight line indicated that second order kinetic model was applicable. The value of  $k_2$  and  $q_e$  were calculated from the intercept and slope of the linear plot, respectively (Table 2). Therefore, it was revealed that experimental  $q_e$  (exp) value agreed with the calculated  $q_e$  (cal) value and correlation coefficient ( $r^2$ ) value was nearly equal to unity. The results indicated that the pseudo-second-order adsorption mechanism was predominant and it was

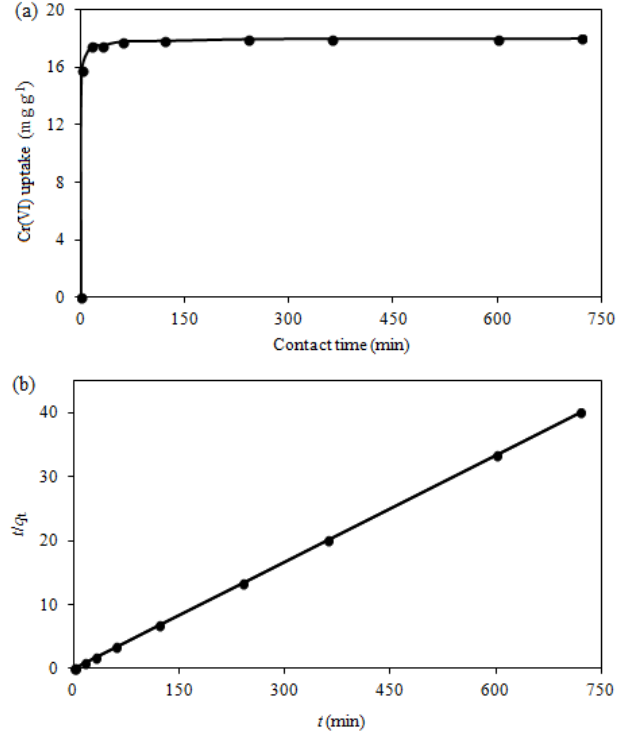


Fig. 5 (a) Effect of contact time and (b) the pseudo-second-order kinetic model for Cr(VI) adsorption on CLSAC (initial Cr(VI) conc.: 100 mg L<sup>-1</sup>; CLSAC conc.: 5.0 g L<sup>-1</sup>; pH: 2.5; agitation speed: 400 rpm, N=3, RSD=<5%)

considered that the rate of the adsorption process was controlled by the chemisorption process for the adsorption of Cr(VI) onto CLSAC.

The intraparticle diffusion model is expressed in Eq. (5):

$$q_t = k_{id} t^{1/2} + c \quad (5)$$

where  $k_{id}$  (mg g<sup>-1</sup>min<sup>-1/2</sup>) is the rate constant of intraparticle diffusion and  $q_t$  (mg g<sup>-1</sup>) is the amount of adsorption at time  $t$  (min). The value of  $c$  and  $k_{id}$  can be determined the intercept and slope of  $q_t$  versus  $t^{1/2}$  plot, respectively. The value of  $c$ ,  $k_{id}$  and correlation coefficient ( $r^2$ ) were given in Table 2. The  $r^2$  value was not satisfactory. The intraparticle diffusion model could not be accepted as the only rate limiting step for the adsorption of Cr(VI) onto CLSAC due to the deviation ( $c$  value in Table 2) of the plot from the origin. In the light of the kinetic data, it was concluded that the pseudo-second-order kinetic model was suitable for modelling the adsorption of Cr(VI) onto CLSAC.

### 3.4. Effect of CLSAC and initial Cr(VI) concentration

The adsorption process was conducted with initial Cr(VI) concentrations between 100 and 1000 mg L<sup>-1</sup> and CLSAC concentrations between 1.0 and 20.0 g L<sup>-1</sup> at constant values of pH (2.5) and contact time (4.0 h) to investigate the effect of Cr(VI) and CLSAC concentration on the removal of this metal. The experimental results showed that percentage of

Table 2 Kinetic parameters of Cr(VI) adsorption onto CLSAC

$C_o$ (mg L <sup>-1</sup> )	$q_e$ (exp) (mg g <sup>-1</sup> )	Pseudo-first-order			$q_e$ (cal) (mg g <sup>-1</sup> )	Pseudo-second-order		Intraparticle diffusion		
		$q_e$ (cal) (mg g <sup>-1</sup> )	$k_1$ (min <sup>-1</sup> )	$r^2$		$k_2$ (g mg <sup>-1</sup> min <sup>-1</sup> )	$r^2$	$k_{id}$ (mg g <sup>-1</sup> min <sup>-1/2</sup> )	$C$ (mg g <sup>-1</sup> )	$r^2$
100	18.03	1.03	0.0054	0.5579	18.01	0.0733	0.9999	0.0416	17.012	0.4236

Cr(VI) adsorption increased by increasing CLSAC concentration even though the amount of Cr(VI) adsorbed by per gram of CLSAC decreased (Fig. 6(a)) because the available adsorption sites or functional groups increased with more adsorbent present, and the interactions may also take place between adsorbent and metal ions as the amount of adsorbent decreases at certain metal ion concentration (Wang *et al.* 2013). Besides, the amount of Cr(VI) uptake increased by increasing the initial Cr(VI) concentration although adsorption percentages decreased with increase in the Cr(VI) concentration (Fig. 6(b)). The initial metal ion concentration plays a role as a driving force to overcome mass transfer resistance for metal ion transportation between the aqueous and solid phases. However, the metal ion adsorption is restricted by saturation of the available active sites on the surface functional groups and thus further metal ion uptake is prevented.

### 3.5 Adsorption isotherms

In present study, two widely accepted isotherm models (Langmuir and Freundlich) were used to describe the relationship between adsorbed Cr(VI) and its equilibrium concentration in solution. These models help to identify the mechanism of adsorption process by providing enough physicochemical information. The Langmuir model assumes that the adsorbent surface is homogeneous, and the uptake of adsorbate molecules occurs on a homogenous surface by monolayer adsorption without any interaction between adsorbed molecules (Deng *et al.* 2009). The linearized Langmuir model equation is expressed in Eq. (6):

$$\frac{C_e}{q_e} = \frac{C_e}{q_{max}} + \frac{1}{b q_{max}} \quad (6)$$

where  $q_e$  (mg g<sup>-1</sup>) is the equilibrium metal ion concentration on the adsorbent;  $C_e$  (mg L<sup>-1</sup>) is the equilibrium metal concentration in the solution;  $q_{max}$  (mg g<sup>-1</sup>) is the maximum monolayer adsorption capacity of the adsorbent and  $b$  (L mg<sup>-1</sup>) is the Langmuir constant related to the free energy or net enthalpy of adsorption. The constants  $q_{max}$  and  $b$  can be evaluated from the slope and intercept of  $C_e/q_e$  versus  $C_e$  linear plot, respectively.

The essential characteristics of Langmuir isotherm model can be described in terms of a dimensionless constant separation factor or equilibrium parameter  $R_L$  (Xu *et al.* 2018) defined in Eq. (7):

$$R_L = \frac{1}{1 + b C_o} \quad (7)$$

where  $C_o$  (mg L<sup>-1</sup>) is the initial amount of adsorbate and  $b$  (L mg<sup>-1</sup>) is the Langmuir constant. The  $R_L$  parameter is

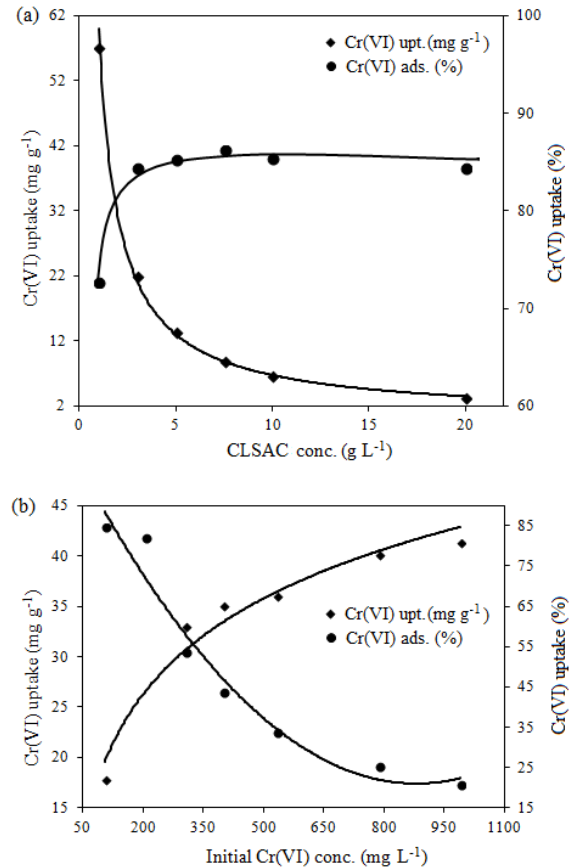


Fig. 6 (a) Effect of adsorbent dosage on the adsorption of Cr(VI) (initial Cr(VI) conc.: 100 mg L<sup>-1</sup>; CLSAC conc.: 1.0–20.0 g L<sup>-1</sup>; pH: 2.5; agitation speed: 400 rpm) and (b) effect of initial Cr(VI) concentration on the adsorption of Cr(VI) (initial Cr(VI) conc.: 100–1000 mg L<sup>-1</sup>; contact time: 4.0 h; CLSAC conc.: 5.0 g L<sup>-1</sup>; pH: 2.5; agitation speed: 400 rpm, N=3, RSD=<5%)

used to predict whether an adsorption system is ‘favorable’ or ‘unfavorable’. The adsorption process as a function of  $R_L$  may be described as  $R_L > 1$ ; unfavorable,  $R_L = 1$ ; Linear,  $0 < R_L < 1$ ; favorable and  $R_L = 0$ ; irreversible.

Freundlich model is suitable for non-ideal sorption on heterogeneous surfaces and multilayer sorption. The heterogeneity is caused by the presence of different functional groups on the surface, and various adsorbent–adsorbate interactions (Deng *et al.* 2009). The linearized Freundlich model equation is described in Eq. (8):

$$\ln q_e = \ln K_f + \frac{1}{n} \ln C_e \quad (8)$$

where  $K_f$  (mg g<sup>-1</sup>) and  $n$  are Freundlich constants related to adsorption capacity and intensity, respectively. These constants  $K_f$  and  $1/n$  are determined from linear plot of  $\ln q_e$  versus  $\ln C_e$ .

Table 3 Langmuir and Freundlich isotherm constants and correlation coefficients for Cr(VI) adsorption onto CLSAC

Langmuir model constants		
$q_{max}$ (mg g <sup>-1</sup> )	$b$ (L mg <sup>-1</sup> )	$r^2$
41.67	0.04	0.996
Freundlich model constants		
$K_f$ (mg g <sup>-1</sup> )	$n$	$r^2$
13.94	5.93	0.730

The calculated constant and correlation coefficient result for both isotherm models were listed in Table 3. As can be seen from the results, the adsorption pattern of Cr(VI) on CLSAC was fitted better with the Langmuir isotherm model ( $r^2 = 0.996$ ) as compared to the Freundlich model ( $r^2 = 0.730$ ) under studied conditions (Table 3, Fig. 7(a) and (b)). The maximum adsorption capacity ( $q_{max}$ ) of CLSAC calculated from Langmuir isotherm equation was found to be 41.67 mg g<sup>-1</sup> and compared with those of other adsorbents reported in the literature (Table 4). Furthermore, the Freundlich constant  $n$  was greater than 1 confirming the favorable adsorption of Cr(VI) onto CLSAC. In addition, calculated the  $R_L$  values for the initial Cr(VI) concentration in the range of 100–1000 mg L<sup>-1</sup> at a constant CLSAC concentration (5.0 g L<sup>-1</sup>) were in the range of 0.023 and 0.183 (Fig. 7(c)). In the light of this result, it was also concluded that the adsorption of Cr(VI) onto CLSAC was favorable.

### 3.6 Effect of temperature and thermodynamic parameters of adsorption

In order to investigate the effect of the temperature on the removal efficiency, the adsorption experiments were conducted with CLSAC concentration of 5.0 g L<sup>-1</sup> and initial Cr(VI) concentration of 100 mg L<sup>-1</sup> at pH 2.0 in the temperature range from 5 to 40 °C. The adsorption of Cr(VI) onto CLSAC decreased from 7.60 mg g<sup>-1</sup> (78.77% removal) to 6.37 mg g<sup>-1</sup> (65.95% removal) when the temperature was increased from 5 to 40 °C, indicating that Cr(VI) uptake was favored at lower temperatures (Fig. 8(a)). The decrease in the adsorption capacity with increasing temperature may be due to the weakening of the adsorptive forces between the active sites on the adsorbent and adsorbate species, and between the adjacent molecules on the adsorbed phase. Bayazit and Kerkez (Bayazit and Kerkez 2014) achieved similar results of Cr(VI) adsorption by modified activated carbon.

The thermodynamic parameters; the Gibbs free energy change ( $\Delta G^\circ$ ), enthalpy change ( $\Delta H^\circ$ ) and entropy change ( $\Delta S^\circ$ ), was calculated to examine the feasibility of the adsorption process.  $\Delta G^\circ$  is expressed in Eq. (9):

$$\Delta G^\circ = -RT \ln K_d \quad (9)$$

where  $R$  is the universal gas constant (8.314 J mol<sup>-1</sup> K<sup>-1</sup>),  $T$  is the temperature (K), and  $K_d$  is the distribution coefficient.  $K_d$  is determined using Eq. (10):

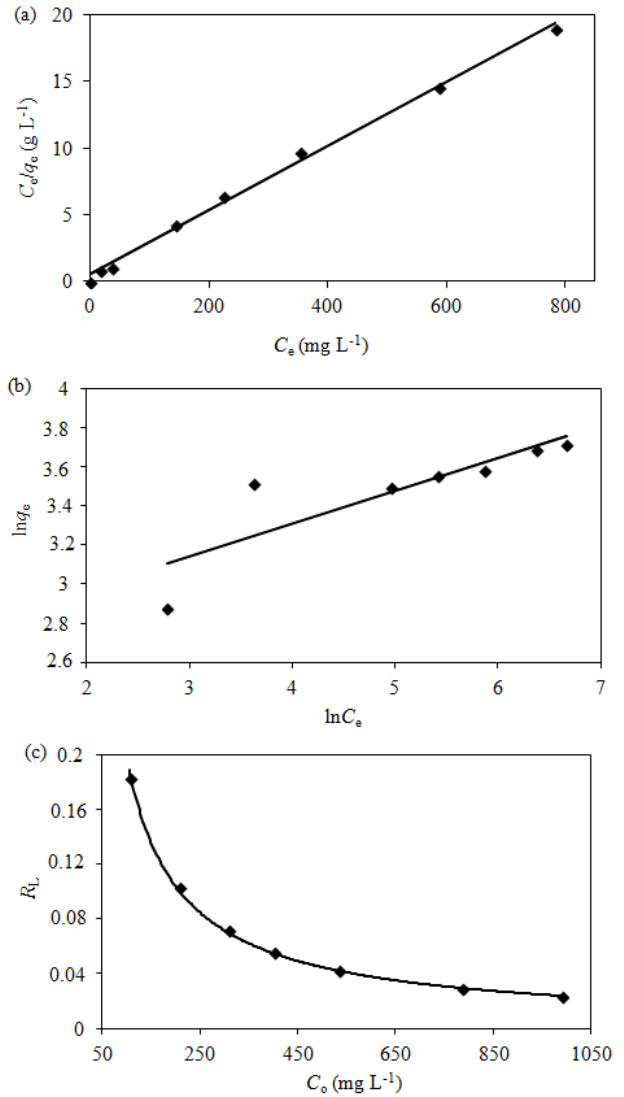


Fig. 7 (a) Langmuir isotherm model, (b) Freundlich isotherm model and (c)  $C_o$  versus  $R_L$  graph (initial Cr(VI) conc.: 100–1000 mg L<sup>-1</sup>; contact time: 4.0 h; CLSAC conc.: 5.0 g L<sup>-1</sup>; pH: 2.5; agitation speed: 400 rpm, N=3, RSD=<5%)

$$K_d = \frac{q_e}{C_e} \quad (10)$$

where  $q_e$  (mg L<sup>-1</sup>) and  $C_e$  (mg L<sup>-1</sup>) are the equilibrium concentration of Cr(VI) on adsorbent and in the solution, respectively.

$\Delta H^\circ$  and  $\Delta S^\circ$  are calculated from Eq. (11):

$$\Delta G^\circ = \Delta H^\circ - T \Delta S^\circ \quad (11)$$

Eq. (12) can be written as:

$$\ln K_d = \frac{\Delta S^\circ}{R} - \frac{\Delta H^\circ}{RT} \quad (12)$$

Thermodynamic parameters,  $\Delta H^\circ$  and  $\Delta S^\circ$ , were calculated from the slope and intercept of the Van't Hoff plot ( $\ln K_d$  vs.  $1/T$ ) shown in Fig. 8(b). The calculated values

Table 4 Comparison of adsorption capacity of CLSAC for Cr(VI) with that of different reported adsorbents

Adsorbent	Adsorption capacity (mg g <sup>-1</sup> )	Reference
3-MPA coated SPION	45.0	(Burks <i>et al.</i> 2014)
PAN-NH <sub>2</sub> nanofibers	137.6	(Avila <i>et al.</i> 2014)
Carbon/AlOOH	25.64	(Kumar <i>et al.</i> 2014)
Magnetic silica with quaternary ammonium salt	26.81	(Yao <i>et al.</i> 2014)
Corncob activated carbon	9.85	(Li <i>et al.</i> 2018)
Sawdust	8.3	(Gupta <i>et al.</i> 2010)
Carbon slurry	15.2	(Gupta <i>et al.</i> 2010)
Granular activated carbon	7.0	(Di Natale <i>et al.</i> 2007)
Magnetite nanoparticles	19.2	(Yuan <i>et al.</i> 2010)
Fe <sub>3</sub> O <sub>4</sub> coated Polypyrrole	238.1	(Bhaumik <i>et al.</i> 2011)
Activated alumina	25.57	(Bhattacharya <i>et al.</i> 2008)
Fly ash	23.86	(Bhattacharya <i>et al.</i> 2008)
Coconut shell	18.69	(Singha and Das 2011)
Mesoporous carbon nitride	48.31	(Chen <i>et al.</i> 2014)
CLSAC	41.67	This study

Table 5 Thermodynamic parameters of Cr(VI) adsorption onto CLSAC at different temperatures

T (K)	$\Delta G^\circ$ (kJ mol <sup>-1</sup> )	$\Delta S^\circ$ (Jmol <sup>-1</sup> K <sup>-1</sup> ) <sup>a</sup>	$\Delta H^\circ$ (kJ mol <sup>-1</sup> ) <sup>a</sup>
278	-3.03		
288	-2.59		
298	-2.06	-38.52	-13.68
313	-1.72		

<sup>a</sup> Measured between 278 and 313 K.

of  $\Delta G^\circ$ ,  $\Delta H^\circ$  and  $\Delta S^\circ$  for the adsorption of Cr(VI) onto CLSAC at different temperature are given in Table 5. The obtained negative values of  $\Delta G^\circ$  indicated that the adsorption of Cr(VI) on the surface of CLSAC was a feasible and spontaneous adsorption process. The decreasing trend in  $\Delta G^\circ$  values with increase in temperature showed the diminishing of the spontaneous of the process and thus the adsorption was not favorable at higher temperatures. The negative value of  $\Delta H^\circ$  indicated that the adsorption of Cr(VI) has exothermic nature. The negative  $\Delta S^\circ$  value showed the decreased randomness at the solid/liquid interface during the adsorption of Cr(VI) onto CLSAC.

### 3.7. Salt Effect on the adsorption yields of Cr(VI)

Waters (natural and waste) contain a variety of different electrolyte types having important effects on the adsorption process so it is essential to investigate the effects of salts on

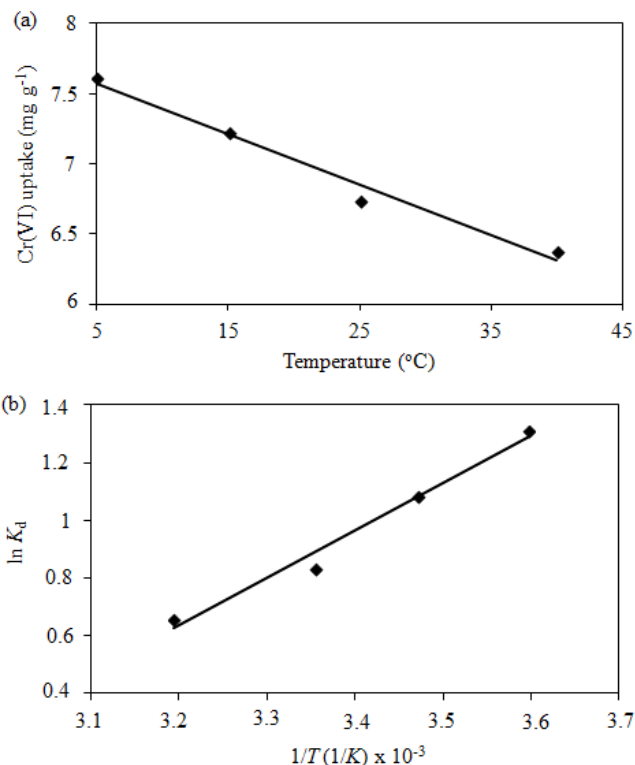


Fig. 8 (a) Effect of temperature on Cr(VI) uptake and (b)  $\ln K_d$  versus  $1/T$  plot for obtaining the thermodynamic parameters (pH: 2.5, initial Cr(VI) conc.: 100 mg L<sup>-1</sup>, CLSAC conc.: 5.0 g L<sup>-1</sup>, contact time: 4.0 h, N=3, RSD=<5%)

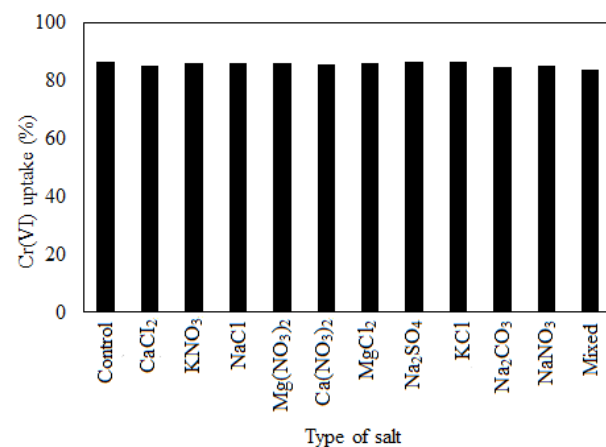


Fig. 9 Effect of salts on Cr(VI) uptake by CLSAC (initial pH: 2.5; CLSAC conc.: 5.0 g L<sup>-1</sup>; initial Cr(VI) and salt concentrations: 100 mg L<sup>-1</sup> of each, N=3, RSD=<5%)

the uptake of Cr(VI) from aqueous solutions. Adsorption studies were carried out by adding 100 mg L<sup>-1</sup> of CaCl<sub>2</sub>, KNO<sub>3</sub>, NaCl, Mg(NO<sub>3</sub>)<sub>2</sub>, Ca(NO<sub>3</sub>)<sub>2</sub>, MgCl<sub>2</sub>, Na<sub>2</sub>SO<sub>4</sub>, KCl, Na<sub>2</sub>CO<sub>3</sub>, NaNO<sub>3</sub> and a mixture of these salt solutions, individually, in 100 mg L<sup>-1</sup> of Cr(VI) solution containing 5.0 g L<sup>-1</sup> of CLSAC and the present adsorption process was applied to these solutions. The results were given in Fig. 9. As can be seen, presence of these salts did not cause significant interfere effect on the adsorption of Cr(VI).

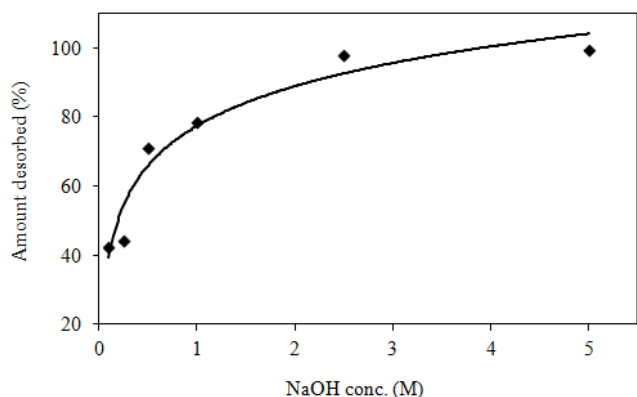


Fig. 10 Effect of NaOH concentration on desorption of Cr(VI) from CLSAC (amount of Cr(VI) adsorbed onto CLSAC:  $10.61 \text{ mg g}^{-1}$ ; volume of NaOH: 10 mL,  $N=3$ ,  $RSD < 5\%$ )

### 3.8. Reusability of CLSAC

The adsorption–desorption cycles were repeated for five times using same preparations to evaluate the reutilization of CLSAC. In these tests, 10 mL of an aqueous solution containing 1 g of Cr(VI) was treated with  $5.0 \text{ g L}^{-1}$  of CLSAC suspension. The concentration of Cr(VI) ions was determined after elution with 2.5 M NaOH solution. There was no significant change observed for the adsorption performance of CLSAC after five adsorption–desorption cycle so it can be concluded that CLSAC can be used effectively at least 5 times with repeated elution.

### 3.9. Analytical validation

Each parameter was repeated at least 3 times and the results were averaged. The method (flame atomic absorption spectrometry) applied for the quantitative determination of Cr (VI) ions from aqueous solution was validated with three main analytical parameters: repeatability (precision, relative standard deviations (RSD%)), limit of detection and accuracy. Details were reported in our previous study (Duran *et al.* 2011).

### 3.10. Desorption of Cr(VI)

Desorption studies are carried out to recover the adsorbed metal extracted from the liquid phase and regenerate adsorbents for another cycle of application. In the present study, the desorption of Cr(VI) from CLSAC's surface was tested using NaOH solutions at various concentrations (0.1–5.0 M) in a batch system. The results obtained showed that the desorption efficiency of Cr(VI) increased with the increase of NaOH concentration (Fig. 10). The desorption efficiency reached from 42.5% to 99.2% with increasing NaOH concentration from 0.1 M to 5.0 M. It is thought that ion exchange mechanism plays a significant role in the adsorption process because of the high desorption efficiency. Furthermore, CLSAC can be employed repeatedly in water treatment as the Cr(VI) adsorbed by CLSAC could be easily desorbed.

## 4. Conclusions

The experimental results obtained from CLSAC used for Cr(VI) removal from aqueous solution exhibited that CLSAC could be a promising adsorbent to remove Cr(VI) from waters and wastewaters. After CLSAC was characterized with the FT-IR spectroscopy, SEM, iodine and methylene blue numbers, pore texture, pH of point zero charge ( $\text{pH}_{\text{pzc}}$ ) and elemental analysis, the Cr(VI) removal performance of CLSAC was investigated on the basis of equilibrium, kinetics and thermodynamics parameters.

- The adsorption process was showed pH dependent and the maximum Cr(VI) removal was achieved at pH 2.5.

- The kinetics of Cr(VI) adsorption onto CLSAC followed by pseudo-second-order model. When CLSAC concentration was increased, the equilibrium adsorption capacity ( $\text{mg g}^{-1}$ ) of CLSAC decreased, while the percent removal efficiency increased.

- The adsorption pattern of Cr(VI) on CLSAC was fitted better with the Langmuir isotherm model indicating that exposing of homogeneous distribution in active sites on the surface. Adsorption capacity of CLSAC for Cr(VI) was determined to be  $41.67 \text{ mg g}^{-1}$  from Langmuir isotherm model equation.

- The adsorption of Cr(VI) onto CLSAC decreased as increasing the temperature. The obtained negative values of  $\Delta G^\circ$  and  $\Delta H^\circ$  expressed that the adsorption of Cr(VI) on the surface of CLSAC was feasible and spontaneous, and exothermic nature, respectively. The negative  $\Delta S^\circ$  value also indicated the decreased randomness at the solid/liquid interface during the adsorption of Cr(VI) onto CLSAC.

- At the presence of  $\text{CaCl}_2$ ,  $\text{KNO}_3$ ,  $\text{NaCl}$ ,  $\text{Mg}(\text{NO}_3)_2$ ,  $\text{Ca}(\text{NO}_3)_2$ ,  $\text{MgCl}_2$ ,  $\text{Na}_2\text{SO}_4$ ,  $\text{KCl}$ ,  $\text{Na}_2\text{CO}_3$ ,  $\text{NaNO}_3$  salts, these salts did not cause significant interfere effect on the adsorption of Cr(VI).

- The desorption efficiency of Cr(VI) increased with increasing NaOH concentration.

- Consequently, the results obtained from this study concluded that CLSAC can be successfully used for the removal of Cr(VI) from aqueous solutions.

## Acknowledgement

The authors would like to thank Dr. Yunus Onal for especially the production and characterization of CLSAC.

## References

- Ahmed, S.M., Zhou, B., Zhao, H., Zheng, Y.P., Wang, Y. and Xia, S. (2020), "Preparation, characterization of activated carbon fiber from luffa and its application in CVFCW for rainwater treatment", *Membr. Water Treat.*, **11**(2), 151–158. <http://dx.doi.org/10.12989/mwt.2020.11.2.151>.
- Aliakbari, Z., Younesi, H., Ghoreyshi, A.A., Bahramifar, N. and Heidari, A. (2017), "Sewage sludge-based activated carbon: Its application for hexavalent chromium from synthetic and electroplating wastewater in batch and fixed-bed column adsorption", *Desalin. Water Treat.*, **93**, 61–73. <https://doi.org/10.5004/dwt.2017.21477>.

- Alidokht, L., Khataee, A.R., Reyhanitabar, A. and Oustan, S. (2011), "Reductive removal of Cr(VI) by starch-stabilized FeO nanoparticles in aqueous solution", *Desalination*, **270**, 105–110. <https://doi.org/10.1016/j.desal.2010.11.028>.
- AL-Othman, Z.A., Ali, R. and Naushad, Mu. (2012), "Hexavalent chromium removal from aqueous medium by activated carbon prepared from peanut shell: Adsorption kinetics, equilibrium and thermodynamic studies", *Chem. Eng. J.*, **184**, 238–247. <https://doi.org/10.1016/j.cej.2012.01.048>.
- Ampiauw, R.E., Yaqub, M. and Lee, W. (2019), "Adsorption of microcystin onto activated carbon: A review", *Membr. Water Treat.*, **10**(6), 405–415. <http://dx.doi.org/10.12989/mwt.2019.10.6.405>.
- ASTM D4607-94(1999), Standard Test Method for Determination of Iodine Number of Activated Carbon, Annual Book of ASTM Standards, USA.
- Axtell, N.R., Sternberg, S.K.P. and Claussen, K. (2003), "Lead and nickel removal using *Microspora* and *Lemna minor*", *Bioresour. Technol.*, **89**, 41–48. [https://doi.org/10.1016/S0960-8524\(03\)00034-8](https://doi.org/10.1016/S0960-8524(03)00034-8).
- Avila, M., Burks, T., Akhtar, F., Göthelid, M., Lansåker, P.C., Toprak, M.S., Muhammed, M. and Uheid, A. (2014), "Surface functionalized nanofibers for the removal of chromium (VI) from aqueous solutions", *Chem. Eng. J.*, **245**, 201–209. <https://doi.org/10.1016/j.cej.2014.02.034>.
- Bayazit, Ş.S. and Kerkez, O. (2014), "Hexavalent chromium adsorption on superparamagnetic multi-wall carbon nanotubes and activated carbon composites", *Chem. Eng. Res. Design*, **92**, 2725–2733. <https://doi.org/10.1016/j.cherd.2014.02.007>.
- Benefield, L.D., Judkins, J.P. and Wend, B.L. (1982), *Process Chemistry for Water and Wastewater Treatment*, Prentice Hall, Englewood Cliffs, NJ, USA.
- Bhattacharya, A.K., Naiya, T.K., Mandal, S.N. and Das, S.K. (2008), "Adsorption, kinetics and equilibrium studies on removal of Cr (VI) from aqueous solutions using different low-cost adsorbents", *Chem. Eng. J.*, **137**, 529–541. <https://doi.org/10.1016/j.cej.2007.05.021>.
- Bhaumik, M., Maity, A., Srinivasu, V. and Onyango, M. (2011), "Enhanced removal of Cr(VI) from aqueous solution using polypyrrole/Fe<sub>3</sub>O<sub>4</sub> magnetic nanocomposite", *J. Hazard. Mater.*, **190**, 381–390. <https://doi.org/10.1016/j.jhazmat.2011.03.062>.
- Burks, T., Avila, M., Akhtar, F., Göthelid, M., Lansåker, P.C., Toprak, M.S., Muhammed, M. and Uheid, A. (2014), "Studies on the adsorption of chromium (VI) onto 3-Mercaptopropionic acid coated superparamagnetic iron oxide nanoparticles", *J. Colloid Interface Sci.*, **425**, 36–43. <https://doi.org/10.1016/j.jcis.2014.03.025>.
- Chen, H., Yan, T. and Jiang, F. (2014), "Adsorption of Cr(VI) from aqueous solution on mesoporous carbon nitride", *J. Taiwan Inst. Chem. Eng.*, **45**, 1842–1849. <https://doi.org/10.1016/j.jtice.2014.03.005>.
- Cui, L., Meng, Q., Zheng, J., Wei, X. and Ye, Z. (2013), "Adsorption of Cr(VI) on 1,2- ethylenediamine-aminated macroporous polystyrene particles", *Vacuum*, **89**, 1–6. <https://doi.org/10.1016/j.vacuum.2012.08.012>.
- Cui, Y. and Atkinson, J.D. (2017), "Tailored activated carbon from glycerol: Role of acid dehydrator on physiochemical characteristics and adsorption performance", *J. Mater. Chem. A.*, **5**(32), 16812–16821. <https://doi.org/10.1039/C7TA02898A>.
- Das, C., Patel, P. De, S. and DasGupta, S. (2006), "Treatment of tanning effluent using nanofiltration followed by reverse osmosis", *Sep. Purif. Technol.*, **50**, 291–299. <https://doi.org/10.1016/j.seppur.2005.11.034>.
- Deng, H., Yang, L., Tao, G. and Dai, J. (2009), "Preparation and characterization of activated carbon from cotton stalk by microwave assisted chemical activation – application in methylene blue adsorption from aqueous solution", *J. Hazard. Mater.*, **166**, 1514–1521. <https://doi.org/10.1016/j.jhazmat.2008.12.080>.
- Department of Health and Human Services. (1991), "Toxicological Profile for Chromium, Public Health Services Agency for Toxic substances and Diseases Registry", Washington, DC, USA.
- Di Natale, F., Lancia, A., Molino, A. and Musmarra, D. (2007), "Removal of chromium ions from aqueous solutions by adsorption on activated carbon and char", *J. Hazard. Mater.*, **145**, 381–390. <https://doi.org/10.1016/j.jhazmat.2006.11.028>.
- Duran, C., Ozdes, D., Gundogdu, A., Imamoglu, M. and Senturk, H.B. (2011), "Tea-industry waste activated carbon, as a novel adsorbent, for separation, preconcentration and speciation of chromium", *Anal. Chim. Acta*, **688**, 75–83. <https://doi.org/10.1016/j.aca.2010.12.029>.
- Elmastas, M., Genc, N., Demirtas, I., Aksit, H. and Aboul-Enien, H.Y. (2013), "Isolation and Identification of Functional Components in Seed of Cherry Laurel (*Laurocerasus officinalis* Roem.) and Investigation of Their Antioxidant Capacity", *J. Biolo. Acti. Prod. Nat.*, **3**(2), 115–120. <https://doi.org/10.1080/22311866.2013.817736>.
- Enniya, I., Rghioui, L. and Jourani, A. (2018) "Adsorption of hexavalent chromium in aqueous solution on activated carbon prepared from apple peels", *Sustain. Chem. Phar.*, **7**, 9–16. <https://doi.org/10.1016/j.scp.2017.11.003>.
- Fierro, V., Torne-Fernandez, V., Montane, D. and Celzard, A. (2008), "Adsorption of phenol onto activated carbons having different textural and surface properties", *Micropor. Mesopor. Mater.*, **111**, 276–284. <https://doi.org/10.1016/j.micromeso.2007.08.002>.
- Fraser, G., Pritzker, M.D. and Legge, R.L. (1994), "Development of liquid membrane pertraction for the removal and recovery of chromium from aqueous effluents", *Sep. Sci. Technol.*, **29**, 2097–2116. <https://doi.org/10.1080/01496399408002192>.
- Gode, F. and Pehlivan, E. (2005), "Removal of Cr(VI) from aqueous solution by two Lewatitanion exchange resins", *J. Hazard. Mater.*, **B 119**, 175–182. <https://doi.org/10.1016/j.jhazmat.2004.12.004>.
- Gupta, V.K., Rastogi, A. and Nayak, A. (2010), "Adsorption studies on the removal of hexavalent chromium from aqueous solution using a low cost fertilizer industry waste material", *J. Colloid Inter. Sci.*, **342**, 135–141. <https://doi.org/10.1016/j.jcis.2009.09.065>.
- Hajeeth, T., Sudha, P.N., Vijayalakshmi, K. and Gomathi, T. (2014), "Sorption studies on Cr (VI) removal from aqueous solution using cellulose grafted with acrylonitrile monomer", *Int. J. Biol. Macromol.*, **66**, 295–301. <https://doi.org/10.1016/j.ijbiomac.2014.02.027>.
- Hizal, J. and Apak, R. (2006), "Modeling of cadmium(II) adsorption on kaolinite-based clays in the absence and presence of humic acid", *Appl. Clay Sci.*, **32**, 232–244. <https://doi.org/10.1016/j.clay.2006.02.002>.
- Jung, C., Heo, J., Han, J., Her, N., Lee, S.J., Oh, J., Ryu, J. and Yoon, Y. (2013), "Hexavalent chromium removal by various adsorbents: Powdered activated carbon, chitosan, and single/multi-walled carbon nanotubes", *Sep. Purif. Technol.*, **106**, 63–71. <https://doi.org/10.1016/j.seppur.2012.12.028>.
- Karthik, R. and Meenakshi, S. (2014), "Adsorption study on removal of Cr(VI) ions by polyaniline composite", *Desalin. Water Treat.*, **1**–11. <https://doi.org/10.1080/19443994.2014.909330>.
- Karthiskeyan, T., Rajgopal, S. and Miranda, L.R. (2005), "Chromium (VI) Adsorption from Aqueous Solution by Hevea Brasilinesis Sawdust Activated Carbon", *J. Hazard. Mater.*, **124**, 192–199. <https://doi.org/10.1016/j.jhazmat.2005.05.003>.

- Khalilia, N.R., Campbella, M., Sandib, G. and Golas, J. (2000), "Production of micro- and mesoporous activated carbon from paper mill sludge I. Effect of zinc chloride activation", *Carbon*, **38**, 1905–1915. [https://doi.org/10.1016/S0008-6223\(00\)00043-9](https://doi.org/10.1016/S0008-6223(00)00043-9).
- Kumar, A. and Jena, H.M. (2017), "Adsorption of Cr(VI) from aqueous solution by prepared high surface area activated carbon from Fox nutshell by chemical activation with H<sub>3</sub>PO<sub>4</sub>", *J. Environ. Chem. Eng.*, **5**(2), 2032–2041. <https://doi.org/10.1016/j.jece.2017.03.035>.
- Kumar, R., Ehsan, M. and Barakat, M.A. (2014), "Synthesis and characterization of carbon/AlOOH composite for adsorption of chromium(VI) from synthetic wastewater", *J. Ind. Eng. Chem.*, **20**, 4202–4206. <https://doi.org/10.1016/j.jiec.2014.01.021>.
- Lakshmipathiraj, P., Raju, G.B., Basariya, M.R., Parvathy, S. and Prabhakar, S. (2008), "Removal of Cr(VI) by electrochemical reduction", *Sep. Purif. Technol.*, **60**, 96–102. <https://doi.org/10.1016/j.seppur.2007.07.053>.
- Levankumar, L., Muthukumar, V. and Gobinath, M.B. (2009), "Batch adsorption and kinetics of chromium (VI) removal from aqueous solutions by Ocimum americanum L. seed pods", *J. Hazard. Mater.*, **161**, 709–13. <https://doi.org/10.1016/j.jhazmat.2008.04.031>.
- Li, H., Gao, P., Cui, J., Zhang, F., Wang, F. and Cheng, J. (2018), "Preparation and Cr(VI) removal performance of corn cob activated carbon", *Environ. Sci. Pollut. Res.*, **25**(21), 20743–20755. <https://doi.org/10.1007/s11356-018-2026-y>.
- Mestre, A.S., Pires, J., Nogueira, J.M.F. and Carvalho, A.P. (2007), "Activated carbons for the adsorption of ibuprofen", *Carbon*, **45**, 1979–1988. <https://doi.org/10.1016/j.carbon.2007.06.005>.
- Mohanty, K., Jha, M., Meikap, B.C. and Biswas, M.N. (2005), "Removal of chromium (VI) from dilute aqueous solutions by activated carbon developed from Terminalia arjuna nuts activated with zinc chloride", *Chem. Eng. Sci.*, **60**, 3049–3059. <https://doi.org/10.1016/j.ces.2004.12.049>.
- Morisset, P., Oswald, J.W., Draper, C.R., Pinner, R. and Ehrhardt, R.A. (1955), "Chromium plating", *J. Electrochem. Soc.*, **102**, 143C–144C. <https://doi.org/10.1149/1.2430046>.
- Norouzi, S., Heidari, M., Alipour, V., Rahmiani, O., Fazlzadeh, M., Mohammadi-moghadam, F., Nourmoradi, H., Goudarzi, B. and Dindarloo, K. (2018), "Preparation, characterization and Cr(VI) adsorption evaluation of NaOH-activated carbon produced from Date Press Cake; an agro-industrial waste", *Bioresour. Technol.*, **258**, 48–56. <https://doi.org/10.1016/j.biortech.2018.02.106>.
- Olad, A. and Farshi Azhar, F. (2014), "A study on the adsorption of chromium (VI) from aqueous solutions on the alginate-montmorillonite/polyaniline nanocomposite", *Desalin. Water Treat.*, **52**, 2548–2559. <https://doi.org/10.1080/19443994.2013.794711>.
- Park, S.J. and Jang, Y.S. (2002), "Pore structure and surface properties of chemically modified activated carbons for adsorption mechanism and rate of Cr(VI)", *J. Colloid Interface Sci.*, **249**, 458–463. <https://doi.org/10.1006/jcis.2002.8269>.
- Rao, R.A.K., Ikram, S. and Uddin, M.K. (2014), "Removal of Cr(VI) from aqueous solution on seeds of *Artimisia absinthium* (novel plant material)", *Desalin. Water Treat.*, **1**–14. <https://doi.org/10.1080/19443994.2014.908147>.
- Sardohan, T., Kir, E., Gulec, A. and Cengeloglu, Y. (2010), "Removal of Cr(III) and Cr(VI) through the plasma modified and unmodified ion-exchange membranes", *Sep. Purif. Technol.*, **74**, 14–20. <https://doi.org/10.1016/j.seppur.2010.05.001>.
- Shanmugalingam, A. and Murugesan, A. (2018), "Removal of Hexavalent Chromium by Adsorption on Microwave Assisted Activated Carbon Prepared from Stems of *Leucas Aspera*", *Zeitschrift fur Physikalische Chemie.*, **232** (4), 489–506. <https://doi.org/10.1515/zpch-2017-0998>.
- Singha, B. and Das, S.K. (2011). Biosorption of Cr(VI) ions from aqueous solutions: Kinetics, equilibrium, thermodynamics and desorption studies. *Colloid Surface B*, **84**, 221–232. <https://doi.org/10.1016/j.colsurfb.2011.01.004>.
- Srivastava, V.C., Mall, I.D. and Mishra, I.M., (2008), "Removal of cadmium(II) and zinc(II) metal ions from binary aqueous solution by rice husk ash", *Coll. Surf. A*, **312**, 172–184. <https://doi.org/10.1016/j.colsurfa.2007.06.048>.
- Suganya, S. and Senthil Kumar, P. (2018), "Influence of ultrasonic waves on preparation of active carbon from coffee waste for the reclamation of effluents containing Cr(VI) ions", *J. Indust. Eng. Chem.*, **60**, 418–430. <https://doi.org/10.1016/j.jiec.2017.11.029>.
- Toprak, A. (2020), "Production and characterization of microporous activated carbon from cherry laurel (*Prunus laurocerasus* L.) stone: application of H<sub>2</sub> and CH<sub>4</sub> adsorption", *Biomass Conv. Bioref.*, **10**, 977–986. <https://doi.org/10.1007/s13399-019-00431-3>.
- Vanderheyden, S.R.H., Vanreppelen, K., Yperman, J., Carleer, R. and Schreurs, S. (2018), "Chromium(VI) removal using in-situ nitrogenized activated carbon prepared from Brewers' spent grain", *Adsorption*, **24**(2), 147–156. <https://doi.org/10.1007/s10450-017-9929-7>.
- Vasudevan, S., Lakshmi, J. and Vanathi, R. (2010), "Electrochemical coagulation for chromium removal: Process optimization, kinetics, isotherm and sludge characterization", *Clean*, **38**, 9–16. <https://doi.org/10.1002/clen.200900169>.
- Wang, P., Zhang, R. and Hua, C. (2013), "Removal of chromium (VI) from aqueous solutions using activated carbon prepared from crofton weed", *Des. Water Treat.*, **51**, 2327–2335. <https://doi.org/10.1080/19443994.2012.735402>.
- Wang, Y.-N., Liu, Q., Shu, L., Miao, M.-S., Liu, Y.-Z. and Kong, Q. (2016), "Removal of Cr(VI) from aqueous solution using Fe-modified activated carbon prepared from luffa sponge: kinetic, thermodynamic, and isotherm studies", *Desalin. Water Treat.*, **57**(60), 29467–29478. <https://doi.org/10.1080/19443994.2016.1185745>.
- Xu, S., Liao, W., Zheng, P. and Fan, Y. (2018), "Optimization of H<sub>2</sub>O<sub>2</sub> Modification Conditions of Bamboo-based Activated Carbon by Response Surface Methodology", *IOP Conference Series: Earth and Environmental Science.*, **146** (1), 1–7. <https://doi.org/10.1088/1755-1315/146/1/012073>.
- Yao, W., Rao, P., Du, Y., Zhang, W. and Liu, T. (2014), "Synthesis of magnetic silica with quaternary ammonium salt and its application for chromium (VI) removal", *Desalin. Water Treat.*, **1**–10. <https://doi.org/10.1080/19443994.2014.911115>.
- Yuan, P., Liu, D., Fan, M., Yang, D., Zhu, R., Ge, F., Zhu, J. and He, H. (2010), "Removal of hexavalent chromium [Cr(VI)] from aqueous solutions by the diatomite supported/unsupported magnetite nanoparticles", *J. Hazard. Mater.*, **173**, 614–621. <https://doi.org/10.1016/j.jhazmat.2009.08.129>.
- Yuan, Z., Xu, Z., Zhang, D., Chen, W., Huang, Y., Zhang, T., Tian, D., Deng, H., Zhou, Y. and Sun, Z. (2018), "Mesoporous activated carbons synthesized by pyrolysis of waste polyester textiles mixed with Mg-containing compounds and their Cr(VI) adsorption", *Coll. Surf. A: Physicochem. Eng. Asp.*, **549**, 86–93. <https://doi.org/10.1016/j.colsurfa.2018.04.008>.
- Zhang, Y., Tang, Q., Chen, S., Gu, F. and Li, Z. (2018), "Heavy metal adsorption of a novel membrane material derived from senescent leaves: Kinetics, equilibrium and thermodynamic studies", *Membr. Water Treat.*, **9**(2), 95–104. <https://doi.org/10.12989/mwt.2018.9.2.095>.